

A Novel Class of Rigid-rod Perylene Diimides and Isoindigo Semiconducting Polymers

Yaping Yu, Danlei Zhu, Xiuyuan Zhu, Mahesh Kumar Ravva, Jiayao Duan, Lang Jiang, Zhengke Li, Wan Yue

Table of contents

1. Instruments and Methods.....	S2
2. Synthesis and Characterization.....	S3
3. TGA.....	S9
4. GPC.....	S9
5. CVs of polymers.....	S10
6. DFT calculations.....	S11
7. OFET device fabrication and characterizations.....	S18
8. AFM.....	S19
9. NMR Spectra.....	S19
10. MS spectra.....	S25
11. References.....	S27

1. Instruments and Methods

^1H NMR and ^{13}C NMR spectra were recorded in deuterated solvents on a Bruker AVANCE 400 NMR Spectrometer and a Bruker AVIII 500WB and 600WB NMR Spectrometer. ^1H NMR chemical shifts are reported in ppm downfield from tetramethylsilane (TMS) reference using the residual protonated solvent as an internal standard. Mass spectra (MALDI-TOF-MS) were determined on a Bruker UltiMate3000-timstof Mass Spectrometer.

TGA: The thermal stability of the polymers was analyzed by thermogravimetric analysis (TGA) using a TA Instruments Q50 under a continuous nitrogen purge of 20 mL min^{-1} . The samples were heated from room temperature to $600\text{ }^\circ\text{C}$ with a uniform heating rate of $10\text{ }^\circ\text{C min}^{-1}$.

GPC: Number-average (M_n) and weight-average (M_w) molecular weights were determined with an Agilent Technologies 1200 series GPC in chlorobenzene at $55\text{ }^\circ\text{C}$, using two PL mixed B columns in series, and calibrated against narrow weight-average dispersity ($D_w < 1.10$) polystyrene standards.

UV: Absorption spectra were measured with UV-1601 Shimadzu UV-vis spectrophotometer in a 1-cm quartz cell.

CV: Cyclic voltammetry (CV) was performed with a CHI760E electrochemical workstation using glassy carbon discs as the working electrode, Pt wire as the counter electrode, Ag/AgCl electrode as the reference electrode. 0.1 M tetrabutylammoniumhexafluorophosphate (Bu_4NPF_6) dissolved in acetonitrile was employed as the supporting electrolyte. The plot includes the signal of the ferrocene as an internal potential marker. CH_2Cl_2 was freshly distilled prior to use.

DFT: All geometry optimizations of single, double, and triple repeating oligomers of polymers considered in this study were carried out using B3LYP/6-31G(d,p) with dispersion correction. Furthermore, the electronic properties such as energy levels and excited state energies were calculated using CAM-B3LYP/6-31G(d,p) method.

OFET

Field-effect transistors (FETs) with bottom-gate bottom-contact (BGBC) configuration

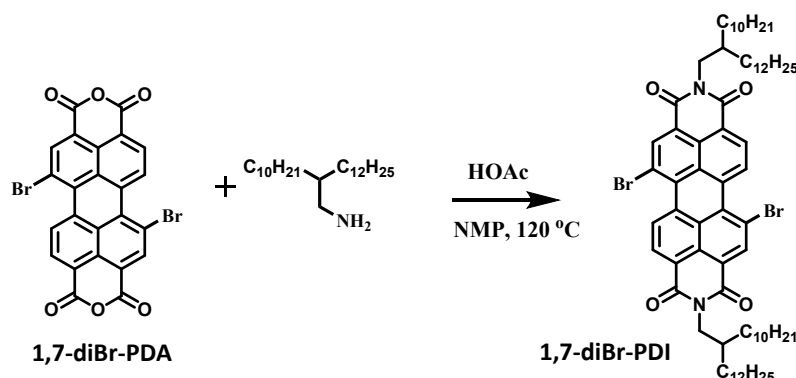
were fabricated on (OTS)-modified SiO₂ (300 nm)/Si substrates to investigate the carrier transport properties of the polymers. The gold drain/source (D/S) electrodes were pre-patterned on the substrates by magnetron sputtering. The substrates were cleaned with pure water, piranha solution (H₂SO₄/H₂O₂ = 7:3), pure water and isopropyl alcohol, and then blown dry with high-purity nitrogen gas. Then the cleaned substrates were treated in the vacuum oven with OTS at 120°C for 2h. For OFETs based on **PB**, **PN** and **PD**, the semiconducting layers were spin-coated on the substrates from chloroform solutions with concentrations of 5 mg mL⁻¹. Electrical characteristics of the devices were recorded with a Keithley 4200-SCS semiconductor parameter analyzer and a Micromanipulator 6150 probe station in glove box.

AFM: Atomic force microscopy (AFM) images were recorded using Cypher ES, Oxford Instruments Asylum Research Inc atomic force microscope in tapping mode under ambient conditions.

2. Synthesis and characterization

All chemicals were purchased from commercial suppliers and used without further purification unless otherwise specified. Regioisomerically pure 1,7-dibromo-substituted Compound (5,12-dibromo-2,9-bis(2-decyltetradecyl)anthra[2,1,9-def:6,5,10-d'e'f]diisoquinoline-1,3,8,10(2H,9H)-tetraone) (**1,7-diBr-PDI**) were synthesized according to the literature.¹ 1-octadecyl-6-(4,4,5,5-tetramethyl-1,3,2-dioxaborolan-2-yl)indoline-2,3-dione (**IS-B**) were synthesized according to the literature.² 3,8-didodecyl-1,3,6,8-tetrahydroindolo[7,6-g]indole-2,7-dione (**IDID**) were synthesized according to the literature.³ Benzo[1,2-b:4,5-b']difuran-2,6(3H,7H)-dione (**Dilactone**) were synthesized according to the literature.⁴ 1,6-dihydronaphtho[1,2-b:5,6-b']difuran-2,7-dione (**NDF**) were synthesized according to the literature.⁵

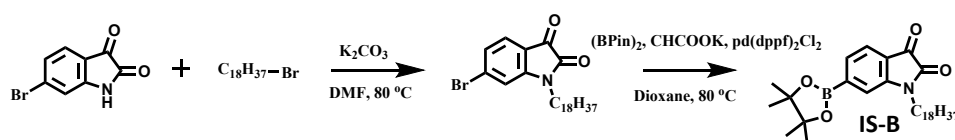
Compound 1,7-diBr-PDI



1,7-dibromoperylene-3,4,9,10-tetracarboxylic bisanhydride (3.0 g, 5.45 mmol) and 2-decyltetradecan-1-amine (4.24 g, 12.0 mmol) was added in NMP (30 mL) and acetic acid (1.5 mL) was heated to 120 °C for 36 h under nitrogen atmosphere. After cooling down, the mixture was poured into water, organic layer was extracted with CH_2Cl_2 , dried over MgSO_4 , and purified by silica gel column chromatography (petroleum ether: $\text{CH}_2\text{Cl}_2 = 1:1$) to give compound **1,7-diBr-PDI** as a red solid (3.5 g, 53 %).

^1H NMR (400 MHz, 298 K, CDCl_3) δ (ppm): 9.43-9.41 (d, $J = 8.2$ Hz, 2H), 8.87 (s, 1H), 8.65-8.63 (d, $J = 8.2$ Hz, 2H), 4.14-4.12 (d, $J = 7.3$ Hz, 2H), 2.01-1.98 (m, 2H), 1.22 (s, 80H), 0.86-0.85 (m, 12H); ^{13}C NMR (100 MHz, 298 K, CDCl_3) δ (ppm): 163.2, 162.8, 138.1, 132.9, 132.8, 130.1, 129.2, 128.5, 127.0, 123.2, 122.8, 120.9, 44.9, 36.7, 32.0, 31.8, 30.1, 29.8, 29.7, 29.4, 26.6, 22.8, 14.2. MS analysis (MALDI-TOF) calculated for $\text{C}_{72}\text{H}_{104}\text{Br}_2\text{N}_2\text{O}_4$ ($\text{M}+\text{H}$) $^+$: 1221.642; found 1221.641.

Compound IS-B

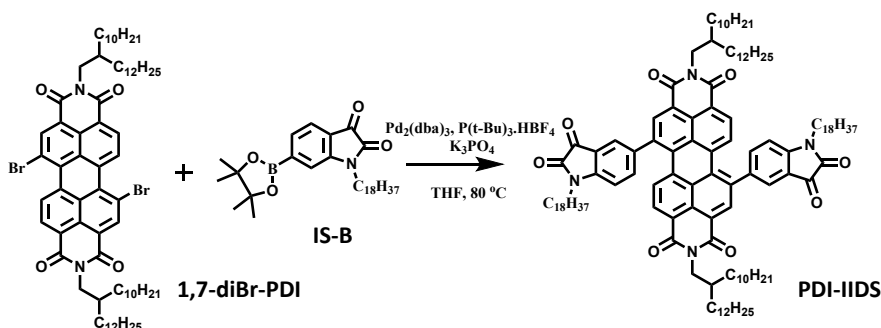


6-bromoindoline-2,3-dione (2.38 g, 10.52 mmol) and K_2CO_3 (1.89 g, 13.67 mmol) was added in DMF (16 mL) was heated to 80 °C for 1 h, then 1-bromooctadecane (4.56 g, 13.68 mmol) was injected in sequence. The reaction mixture was stirred at 80 °C for 4 h. After cooling to room temperature, solvent was removed under reduced pressure and the residue was quickly purified via silica gel column chromatography (DCM) to give

crude product 6-bromo-1-octadecylindoline-2,3-dione, 6-bromo-1-octadecylindoline-2,3-dione (1.7 g, 3.55 mmol), bis(pinacolato)diboron (1.35 g, 5.32 mmol) and $\text{Pd}(\text{dppf})_2\text{Cl}_2$ (130 mg, 0.18 mmol), potassium acetate (697 mg, 7.10 mmol) were added into a glass pressure vessel under nitrogen atmosphere. Then dioxane (25 mL) was added by injection in sequence. The reaction mixture was stirred at 80 °C for 12 h. After cooling down, the mixture was poured into water, organic layer was separated with CH_2Cl_2 , dried over MgSO_4 , and purified by silica gel column chromatography (petroleum ether: $\text{CH}_2\text{Cl}_2 = 1:3$) to give **IS-B** as deep orange solid (1.51 g, 81 %)

^1H NMR (400 MHz, 298 K, CDCl_3) δ (ppm): 7.58-7.54 (br, 2H), 7.26-7.24 (d, $J = 8.1$ Hz, 1H), 3.75-3.71 (m, 2H), 1.73-1.69 (m, 2H), 1.37 (s, 12H), 1.26-1.25 (m, 30H), 0.89-0.85 (m, 3H); ^{13}C NMR (100 MHz, 298 K, CDCl_3) δ (ppm) 184.4, 158.2, 150.1, 130.3, 124.2, 119.5, 115.4, 84.8, 83.6, 40.3, 32.0, 29.8, 29.7, 29.6, 29.4, 29.3, 27.4, 26.9, 25.1, 24.9, 22.8, 14.2. MS analysis (MALDI-TOF) calculated for $\text{C}_{32}\text{H}_{52}\text{BNO}_4$ ($\text{M}+\text{H}$) $^+$: 526.406; found 526.406.

Compound PDI-DIIS

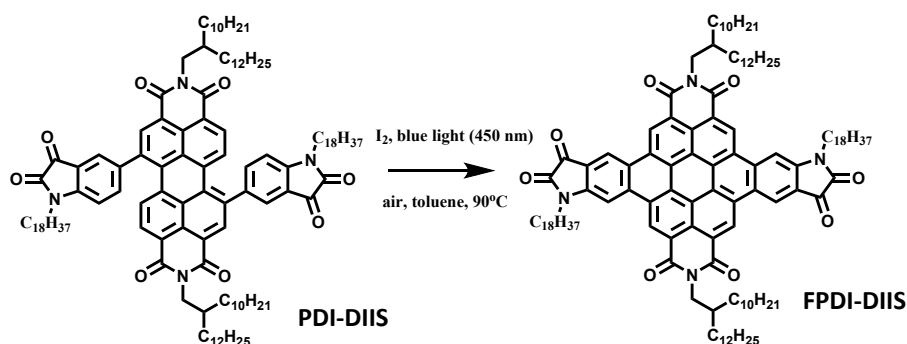


5,12-dibromo-2,9-bis(2-decyltetradecyl)anthra[2,1,9-def:6,5,10-d'e'f']diisoquinoline-1,3,8,10(2H,9H)-tetraone (**1,7-diBr-PDI**) (364 mg, 0.30 mmol), 1-octadecyl-6-(4,4,5,5-tetramethyl-1,3,2-dioxaborolan-2-yl)indolin-2-one (**IS-B**) (344 mg, 0.65 mmol) and $\text{Pd}_2(\text{dba})_3$ (13 mg, 0.014 mmol), $\text{P}(t\text{-Bu})_3\text{BF}_4$ (16.5 mg, 0.057 mmol) were added into a glass pressure vessel under nitrogen atmosphere. Then THF (15 ml) and potassium phosphate (450 mg, 2M) were added by injection in sequence. The reaction mixture was stirred at 80 °C for 10 h. After cooling down, the mixture was poured into water, organic layer was extracted with CH_2Cl_2 , dried over MgSO_4 , and purified by silica gel column chromatography (petroleum ether: $\text{CH}_2\text{Cl}_2 = 1:2$) to give intermediate

product as a purplish red solid **PDI-DIIS** (360 mg, 65 %).

^1H NMR (400 MHz, 298 K, $\text{CDCl}_2\text{CDCl}_2$) δ (ppm): 8.62 (s, 2H), 8.32-8.30 (d, $J = 8.1$ Hz, 2H), 7.92-7.90 (d, $J = 8.1$ Hz, 2H), 7.76-7.66 (m, 2H), 7.36-7.04 (m, 4H), 4.10-4.18 (m, 4H), 3.73-3.62 (m, 4H), 1.97 (s, 2H), 1.63 (s, 22H), 1.21 (s, 136H), 0.86-0.84 (m, 18H); ^{13}C NMR (150 MHz, 298 K, $\text{CDCl}_2\text{CDCl}_2$) δ (ppm) 182.8, 163.2, 163.0, 158.1, 158.0, 152.1, 139.2, 134.1, 133.7, 132.3, 130.8, 130.0, 128.7, 127.9, 127.0, 124.6, 124.4, 122.7, 122.5, 117.0, 116.9, 110.4, 110.2, 58.4, 44.8, 40.4, 40.2, 36.5, 31.8, 30.0, 29.6, 29.6, 29.5, 29.3, 22.6, 14.1. MS analysis (MALDI-TOF) calculated for $\text{C}_{124}\text{H}_{184}\text{N}_4\text{O}_8$: 1858.856; found 1858.413.

Compound FPDI-DIIS

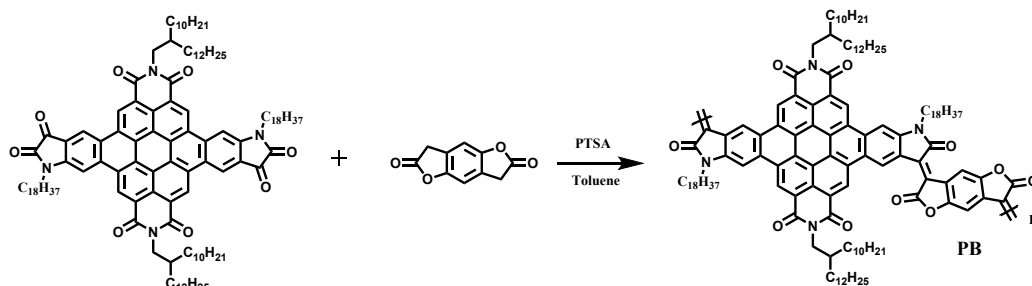


The intermediate product **PDI-DIIS** (50 mg, 0.027 mmol) was dissolved in toluene (20 ml) and I_2 (2.0 mg) was added, this solution was illuminated with blue light ($\lambda = 450$ nm) at 90°C for 12 h by LED flow reactor (WATTCAS, WP-TEC-1020HSL). After removal of the solvent, the residue was purified by silica gel column chromatography (petroleum ether: $\text{CH}_2\text{Cl}_2 = 1:3$) to give compound **FPDI-DIIS** as a brown-red solid (35 mg, 70 %).

^1H NMR (600 MHz, 323 K, CDCl_3) δ (ppm): 9.73 (s, 2H), 9.70 (s, 2H), 9.02 (s, 2H), 8.11 (s, 2H), 4.47-4.46 (m, 4H), 4.19-4.17 (m, 4H), 2.16-2.11 (m, 6H), 1.73-1.71 (m, 4H), 1.61-1.59 (m, 4H), 1.48-1.44 (m, 10H), 1.40-1.38 (m, 6H), 1.30-1.12 (m, 120H), 0.86-0.84 (m, 6H), 0.82-0.76 (m, 12H); ^{13}C NMR (100 MHz, 298 K, CDCl_3) δ (ppm) 163.8, 163.6, 158.2, 148.3, 135.5, 128.1, 126.4, 124.5, 124.1, 123.8, 121.3, 119.3, 102.8, 45.5, 41.2, 37.2, 32.1, 32.0, 31.9, 30.2, 29.8, 29.7, 29.5, 29.4, 27.7, 27.2, 26.8, 22.7, 14.2, 14.1. MS analysis (MALDI-TOF) calculated for $\text{C}_{124}\text{H}_{180}\text{N}_4\text{O}_8$ ($\text{M}+\text{H}$) $^+$: 1855.391; found 1855.394. Elemental analysis calculated for $\text{C}_{124}\text{H}_{180}\text{N}_4\text{O}_8$: C, 80.30;

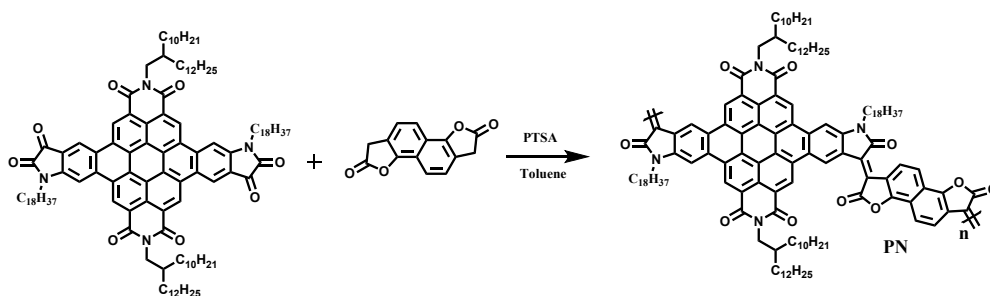
H, 9.78; N, 3.02; O, 6.90. Found: C, 80.17; H, 9.83; N, 2.60; O, 6.85.

PB



FPDI-DIIS (50 mg, 0.03 mmol), benzo[1,2-b:4,5-b']difuran-2,6(3H,7H)-dione (**Dilactone**) (5.70 mg, 0.03 mmol) in toluene (0.5 mL) and p-toluenesulfonic acid monohydrate (1.71 mg, 0.009 mmol) was added. The mixture was stirred at 115°C for 48 h, after which it was precipitated in methanol and filter through a Soxhlet thimble. The polymer was extracted with methanol, hexane, and dichloromethane sequentially, the dichloromethane fraction was concentrated by evaporation, which was then precipitated into methanol and filtered off to give the polymer **PB** (46 mg, 85 %). GPC (CB, 55 °C): $M_n = 13$ kDa, $M_w = 32$ kDa, polydispersity index (PDI) = 2.4. $^1\text{H NMR}$ (500 MHz, 403K, $\text{CDCl}_2\text{CDCl}_2$) δ (ppm): 9.94-9.08 (broad), 5.20-3.90 (broad), 3.11-0.35 (broad). Elemental analysis calculated for $\text{C}_{134}\text{H}_{184}\text{N}_4\text{O}_{10}$: C, 80.03; H, 9.22; N, 2.79; O, 7.96. Found: C, 79.54; H, 9.17; N, 2.49; O, 9.09.

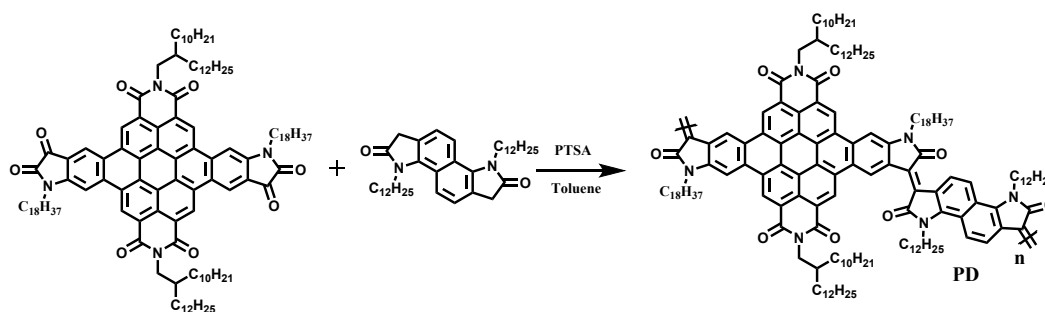
PN



FPDI-DIIS (45 mg, 0.024mmol), 1,6-dihydronaphtho[1,2-b:5,6-b']difuran-2,7-dione (**NDF**) (5.76 mg, 0.024mmol) in toluene (0.5 mL) and p-toluenesulfonic acid

monohydrate (1.37 mg, 0.0072 mmol) was added. The mixture was stirred at 115°C for 36 h, after which it was precipitated in methanol and filter through a Soxhlet thimble. The polymer was extracted with methanol, hexane, and chloroform sequentially, the chloroform fraction was concentrated by evaporation, which was then precipitated into methanol and filtered off to give polymer **PN** (45 mg, 90 %). GPC (CB, 55 °C): $M_n = 16$ kDa, $M_w = 24$ kDa, PDI = 1.5. $^1\text{H NMR}$ (500 MHz, 403K, $\text{CDCl}_2\text{CDCl}_2$) δ (ppm): 11.32-6.19 (broad), 5.23-3.47 (broad), 3.05-0.11 (broad). Elemental analysis calculated for $\text{C}_{138}\text{H}_{186}\text{N}_4\text{O}_{10}$: C, 80.42; H, 9.10; N, 2.72; O, 7.76. Found: C, 80.03; H, 9.09; N, 2.14; O, 8.21.

PD



FPDI-DIIS (56 mg, 0.03 mmol), 3,8-didodecyl-1,3,6,8-tetrahydroindolo[7,6-g]indole-2,7-dione (IDID) (17.36 mg, 0.03 mmol) in toluene (0.5 mL) and p-toluenesulfonic acid monohydrate (1.71 mg, 0.009 mmol) was added. The mixture was stirred at 115°C for 36 h, after which it was precipitated in methanol and filter through a Soxhlet thimble. The polymer was extracted with methanol, hexane, and chloroform sequentially, the chloroform fraction was concentrated by evaporation, which was then precipitated into methanol and filtered off to give polymer **PD** (58 mg, 80 %). GPC (CB, 55 °C): $M_n = 135$ kDa, $M_w = 43$ kDa, PDI = 3.1. $^1\text{H NMR}$ (500 MHz, 403K, $\text{CDCl}_2\text{CDCl}_2$) δ (ppm): 10.09-8.89 (broad), 8.38-7.32 (broad), 5.24-3.96 (broad), 2.80-0.11 (broad). Elemental analysis calculated for $\text{C}_{162}\text{H}_{236}\text{N}_6\text{O}_8$: C, 81.22; H, 9.93; N, 3.51; O, 5.34. Found: C, 80.97; H, 9.99; N, 3.12; O, 5.55.

3. Thermogravimetric Analysis (TGA)

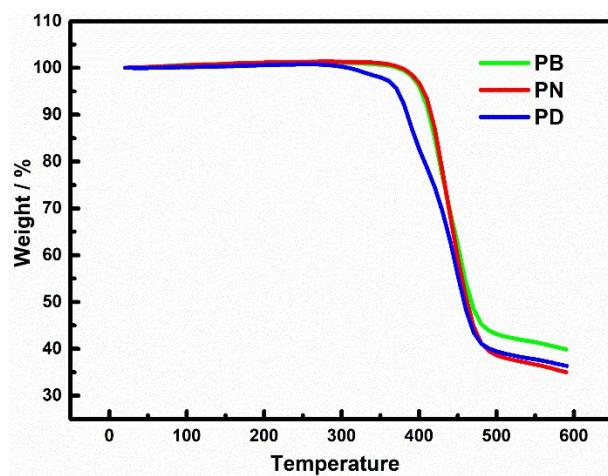
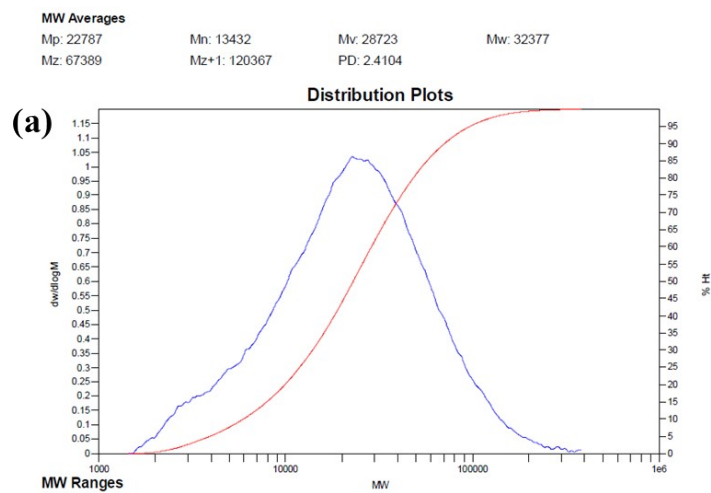


Figure S1: The TGA of polymers.

4. Gel-Permeation Chromatogram (GPC)



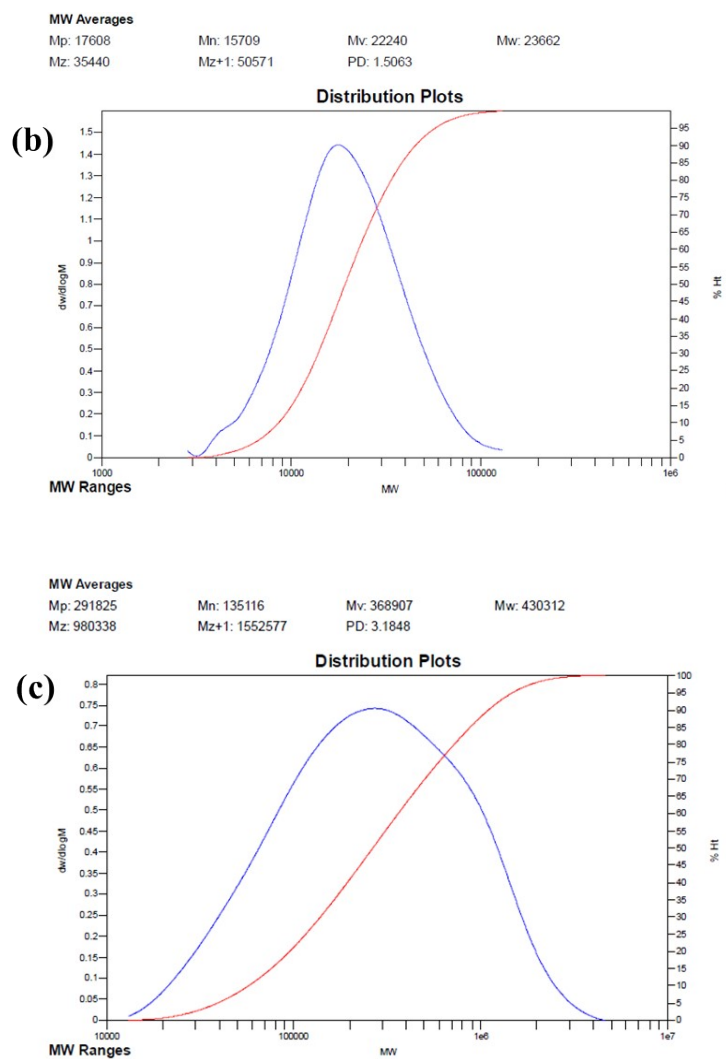
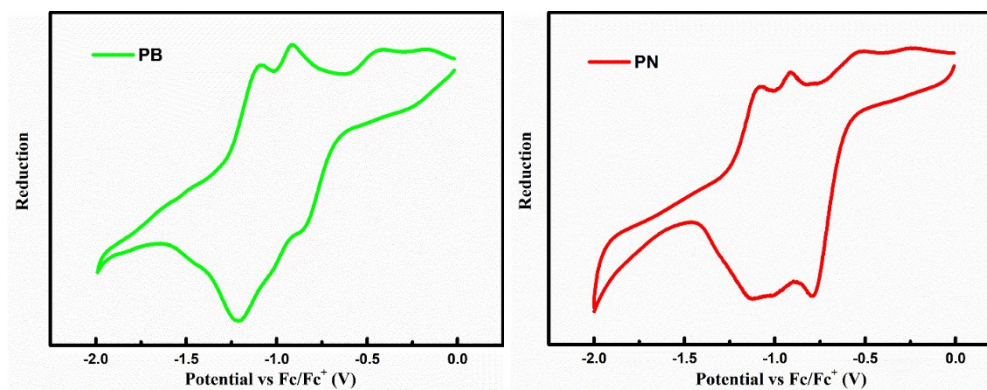


Figure S2. GPC recorded at 55°C with CB as eluent for (a) PB, (b) PN, (c) PD.

5. CVs of polymers



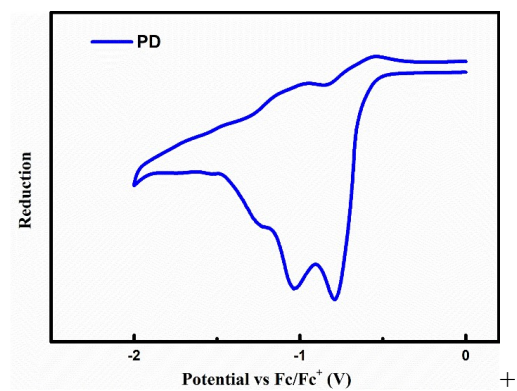
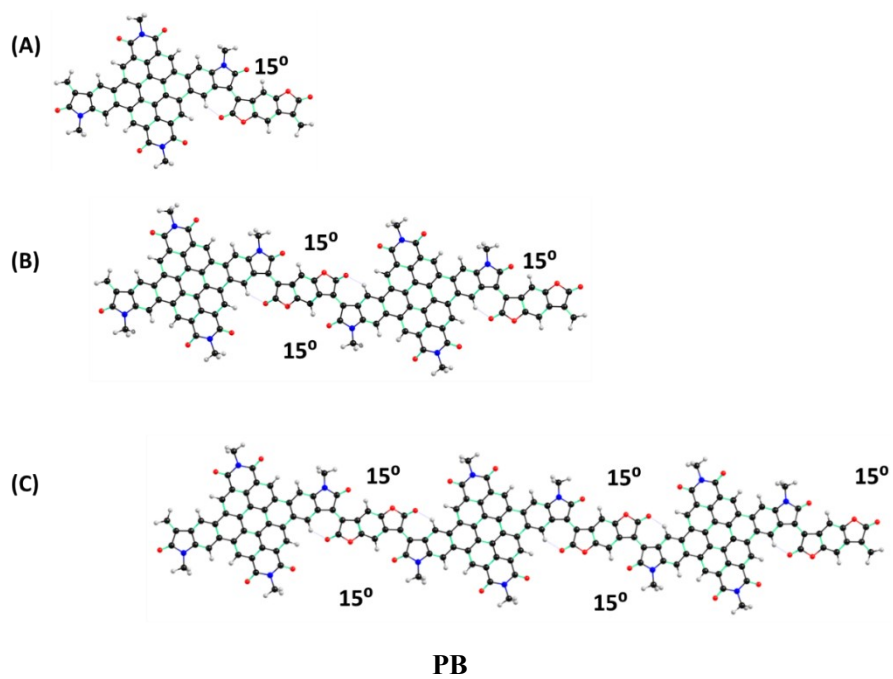


Figure S3: The reductive profiles of polymer **PB**, **PN**, and **PD** in acetonitrile solution (V vs Fc/Fc⁺).

6. DFT calculations



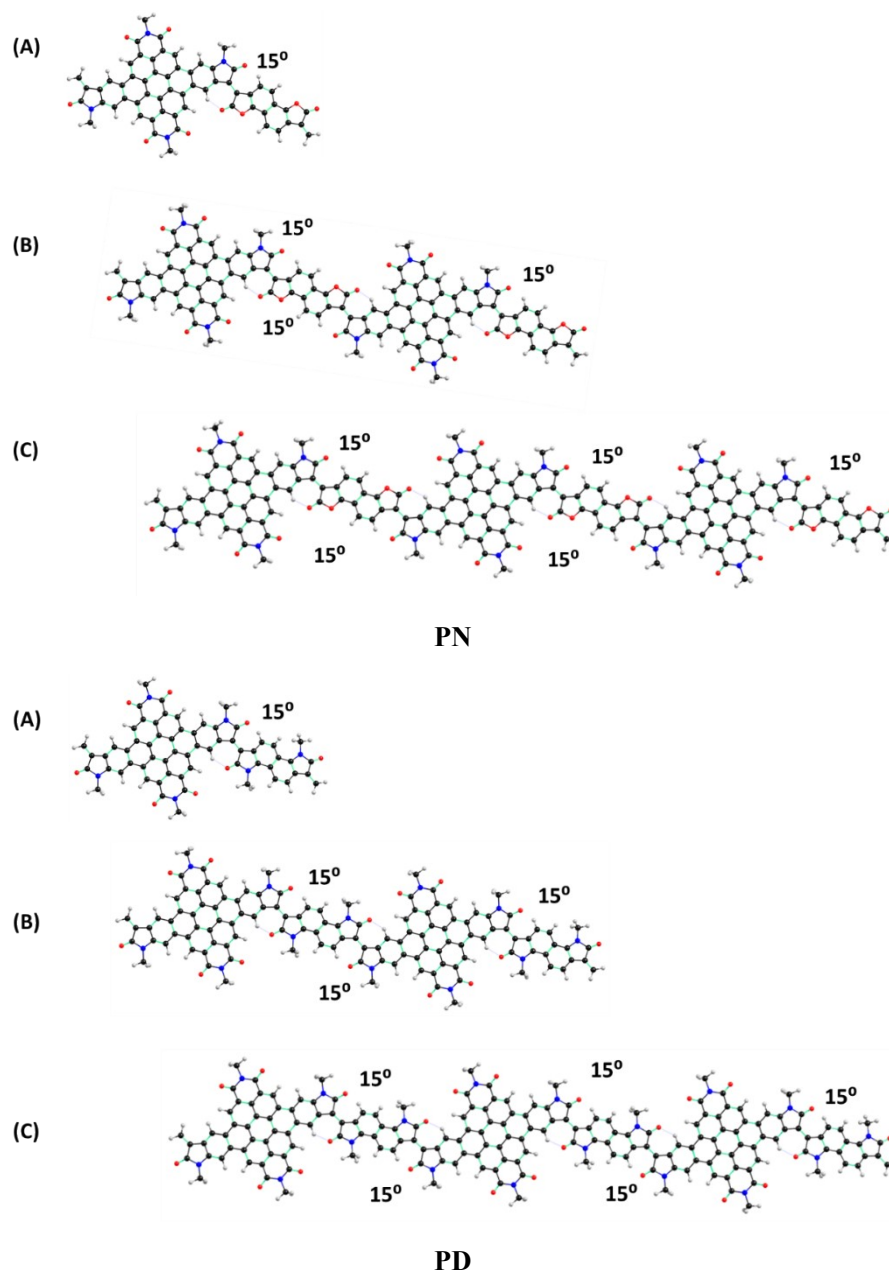


Figure S4: optimized geometries of one (A), two (B), and three (C) repeating units of polymer **PB**, **PN**, and **PD** as determined using B3LYP-D/6-31G(d) method.

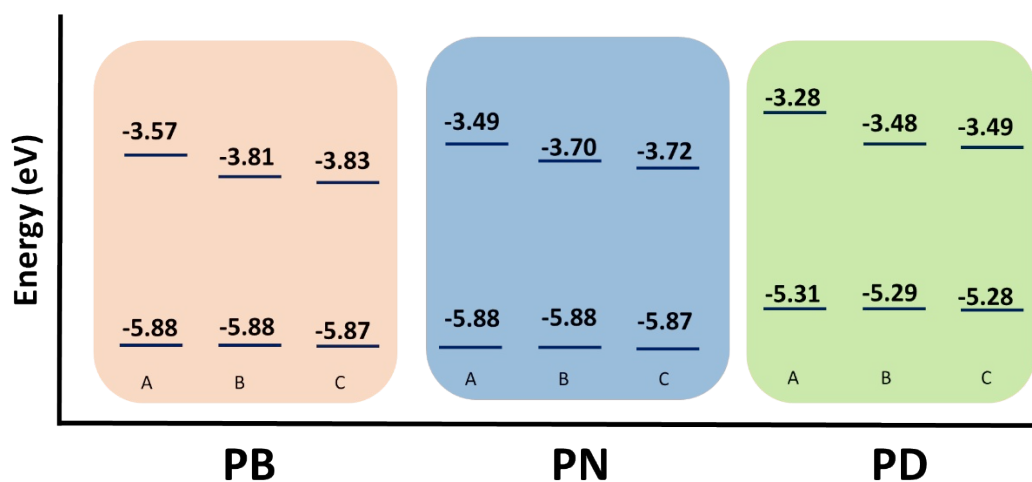


Figure S5: Calculated HOMO and LUMO energy values of **PB**, **PN**, and **PD** oligomers at B3LYP-D/6-31G* level of theory. In each case, one (A), two (B), and three (C) repeating units of oligomers are considered. All values are summarized in Figure S5.

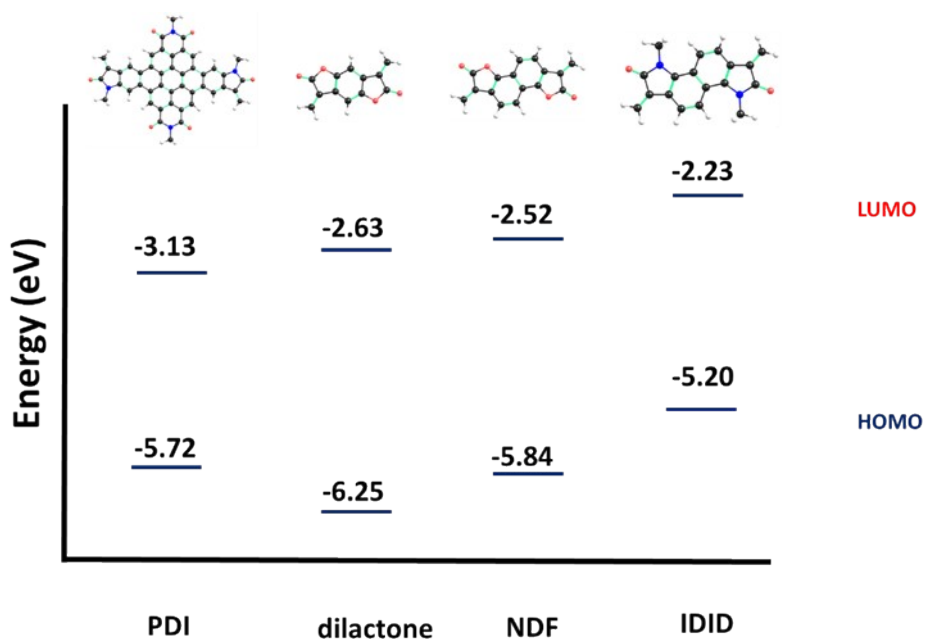


Figure S6: Calculated HOMO and LUMO energies of monomers using B3LYP/6-31G* level of theory.

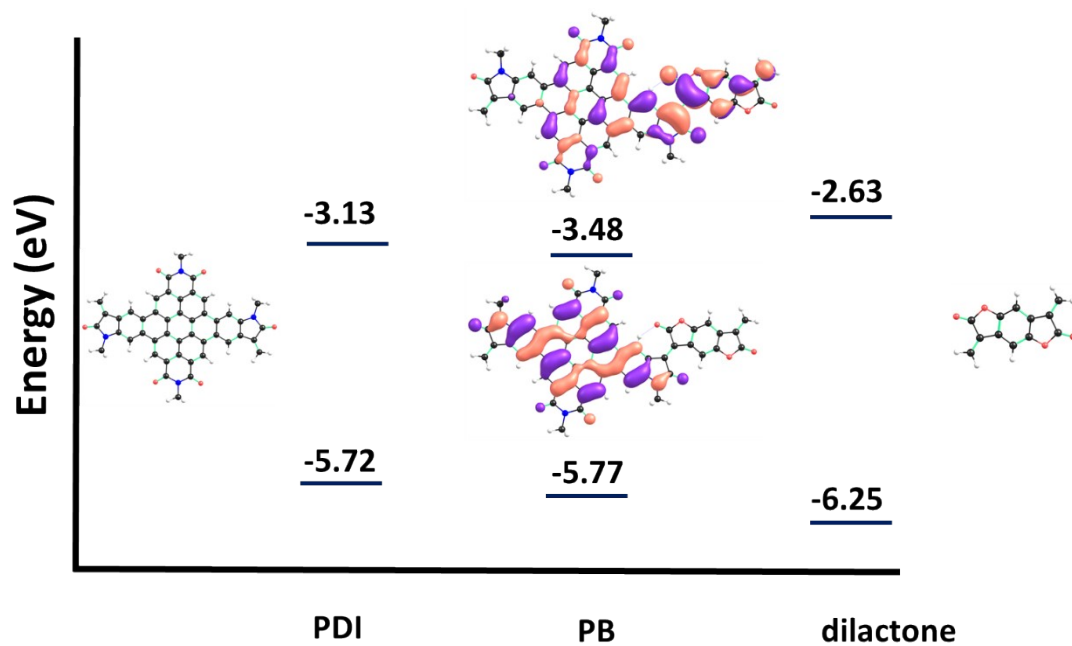


Figure S7: Calculated HOMO and LUMO energies of **PB** and fragments using B3LYP/6-31G* level of theory.

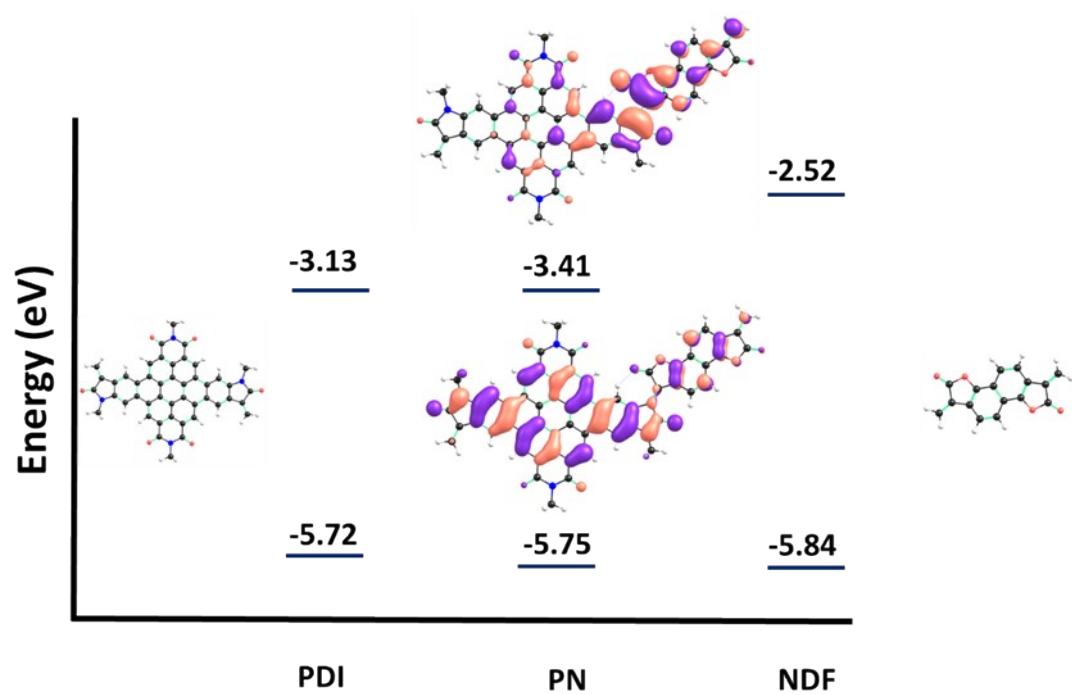


Figure S8: Calculated HOMO and LUMO energies of **PN** and fragments using B3LYP/6-31G* level of theory.

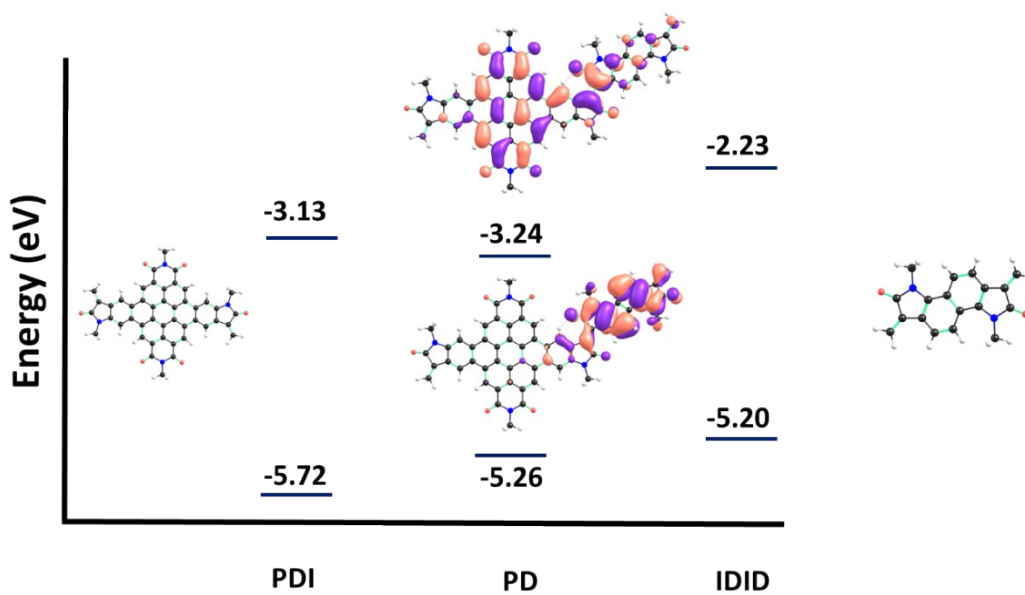


Figure S9: Calculated HOMO and LUMO energies of **PD** and fragments using B3LYP/6-31G* level of theory.

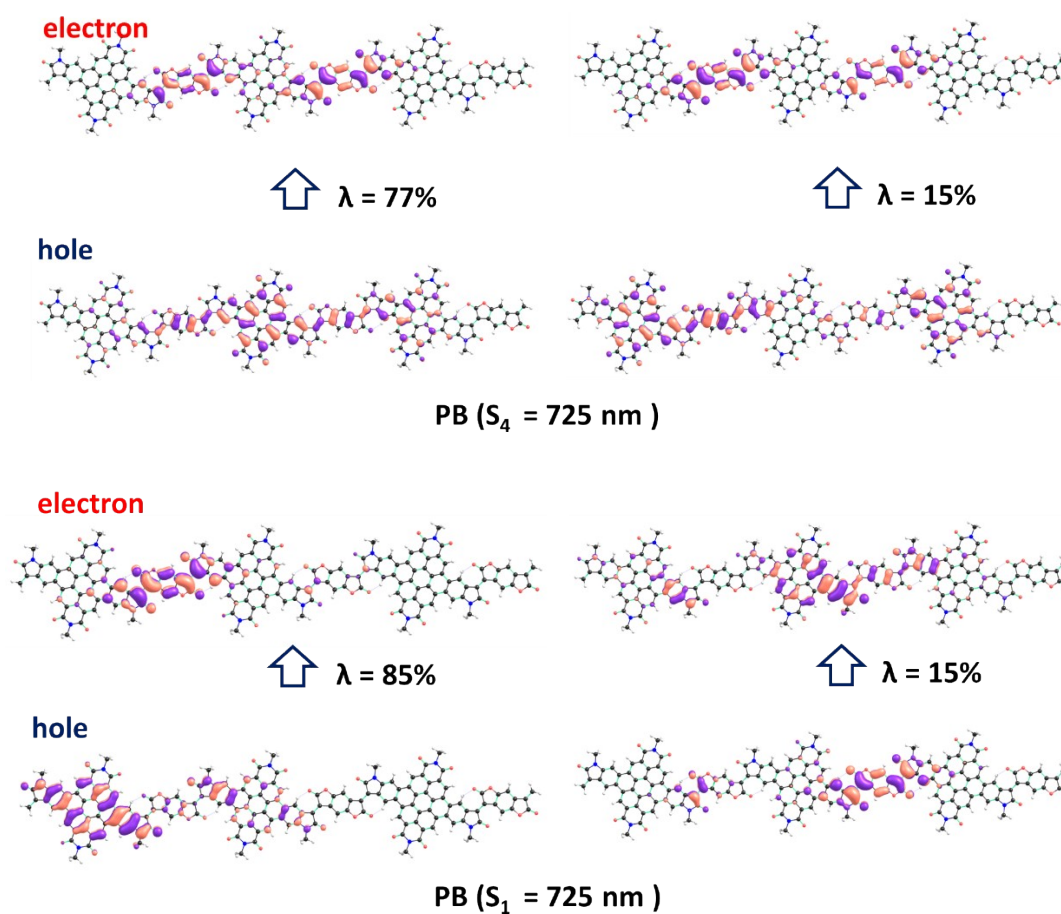


Figure S10: Pictorial representation of hole and electron wavefunctions of first (S_1) and fourth (S_4)

excited-states of three repeating units of **PB** oligomer as obtained by TD-B3LYP-D/6-31G(d) method

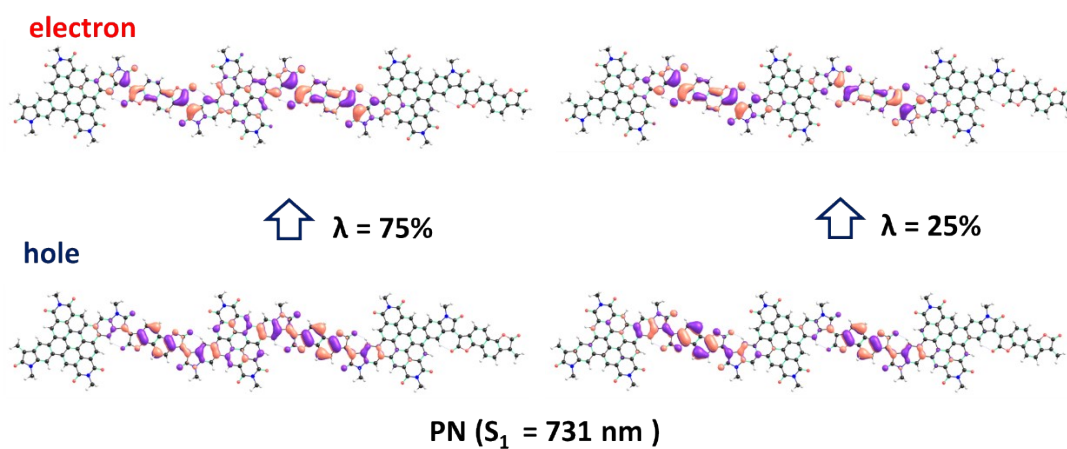


Figure S11: Pictorial representation of hole and electron wavefunctions of first (S_1) excited-states of three repeating units of **PN** oligomer as obtained by TD-B3LYP-D/6-31G(d) method.

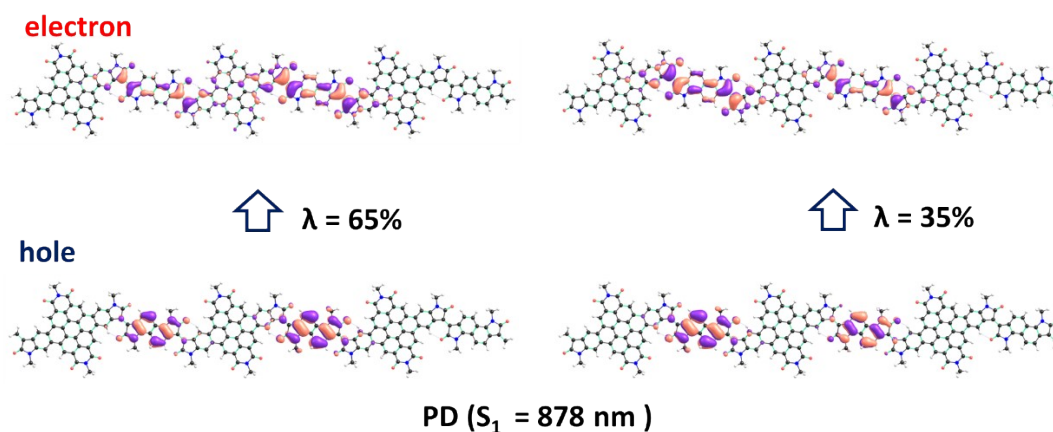


Figure S12: Pictorial representation of hole and electron wavefunctions of first (S_1) excited-states of three repeating units of **PD** oligomer as obtained by TD-B3LYP-D/6-31G(d) method.

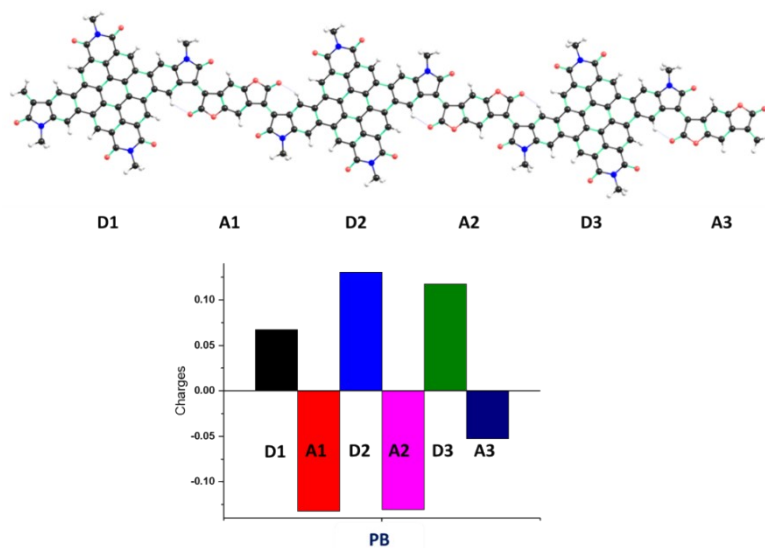


Figure S13: Calculated charge on fragment of **PB** trimer segments using B3LYP/6-31G* level of theory.

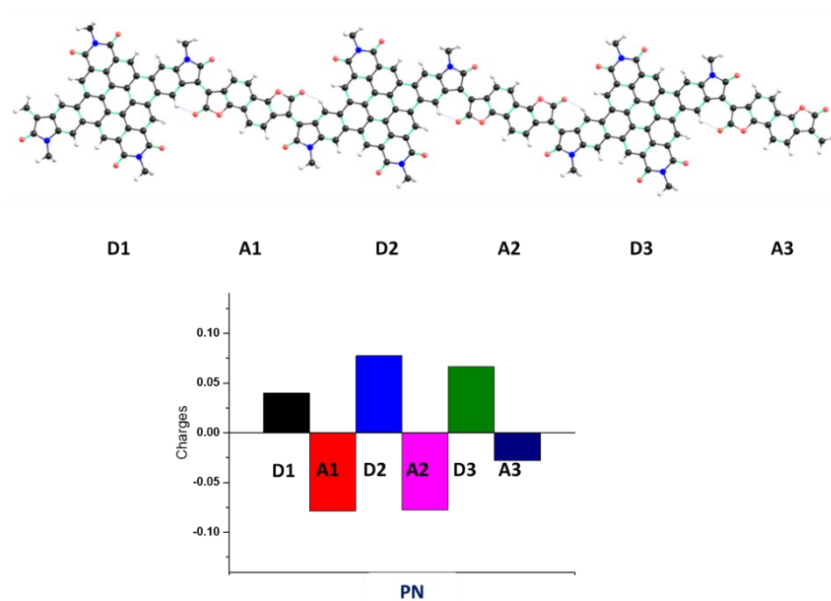


Figure S14: Calculated charge on fragment of **PN** trimer segments using B3LYP/6-31G* level of theory.

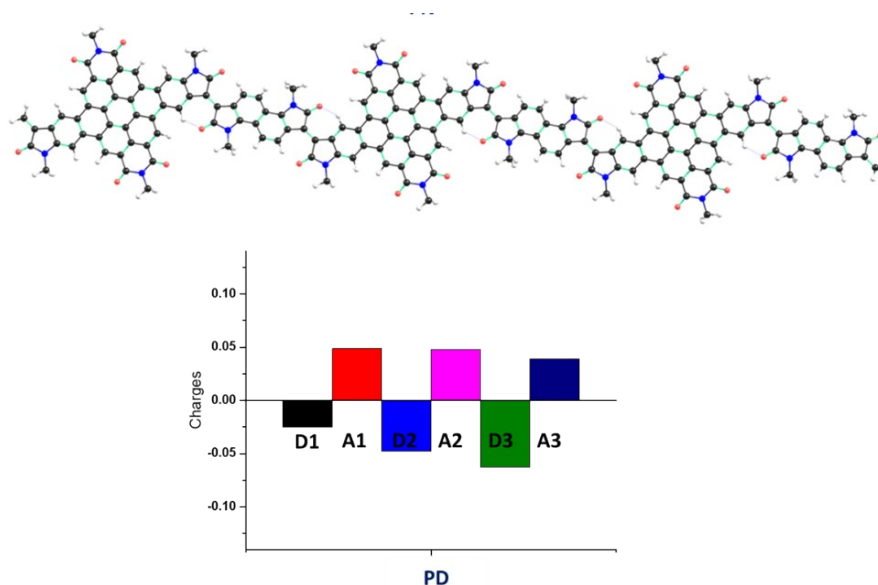


Figure S15: Calculated charge on fragment of **PD** trimer segments using B3LYP/6-31G* level of theory.

7. OFET device fabrication and characterizations

Table S1. The thin-film transistor properties of polymer **PB**, **PD** in a BGTC configuration. The thin films were thermally annealed (TA) for 20 minutes before measurement and all devices were measured under nitrogen atmosphere.

Polymer	Solvent	TA	μ_e [cm ² V ⁻¹ s ⁻¹]	V_T [V]	I_{on}/I_{off}	W/L [μm]
		[°C]				
PD	chloroform	90	8.96×10^{-4}	9	4×10^3	1400/5
	chloroform	120	7.74×10^{-4}	7	2×10^4	1400/20
	chloroform	150	7.42×10^{-4}	6	1×10^3	1400/20
PB	chloroform	90	8.93×10^{-4}	9	2×10^5	1400/10
	chloroform	120	9.63×10^{-4}	-14	4×10^3	1400/10
	chloroform	150	8.23×10^{-4}	7	3×10^4	1400/20

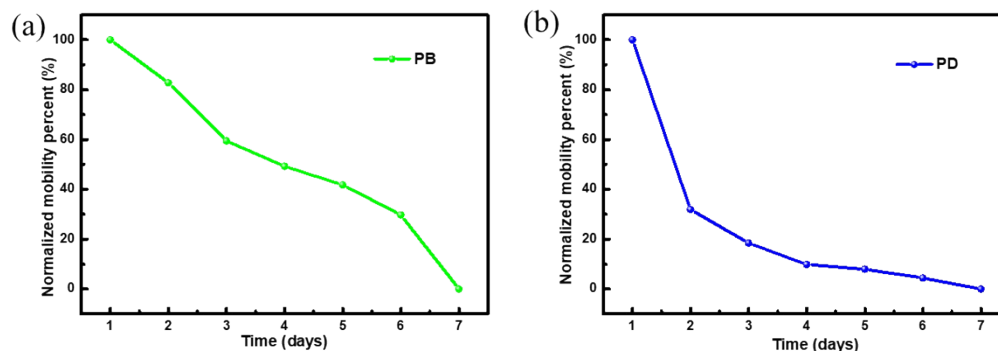


Figure S16: The OFET device stability of polymer (a) **PB** and (b) **PD** in air for seven days.

8. AFM

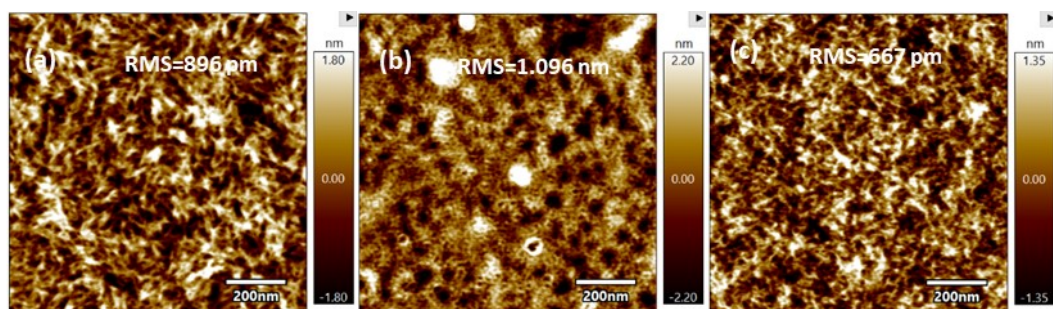


Figure S17: AFM height images of thin films of (a) PB and (b) PN, (c) PD.

9. NMR Spectra

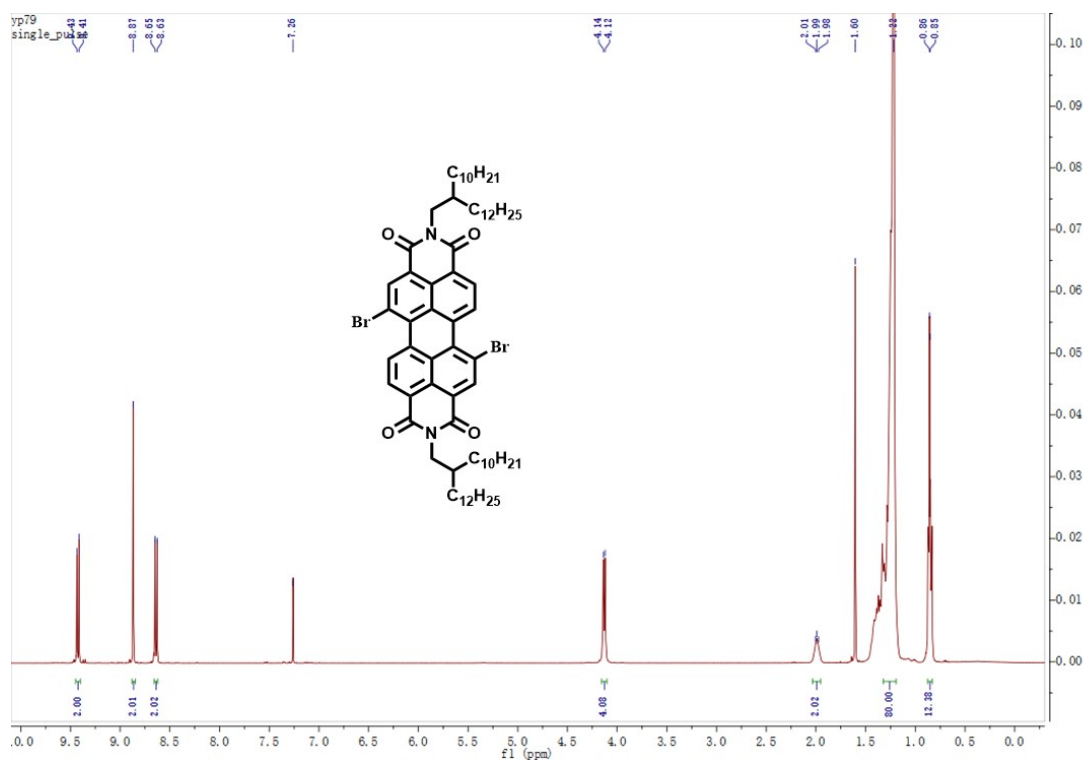


Figure S18: ^1H NMR spectrum of 1,7-diBr-PDI in CDCl_3 at 298 K.

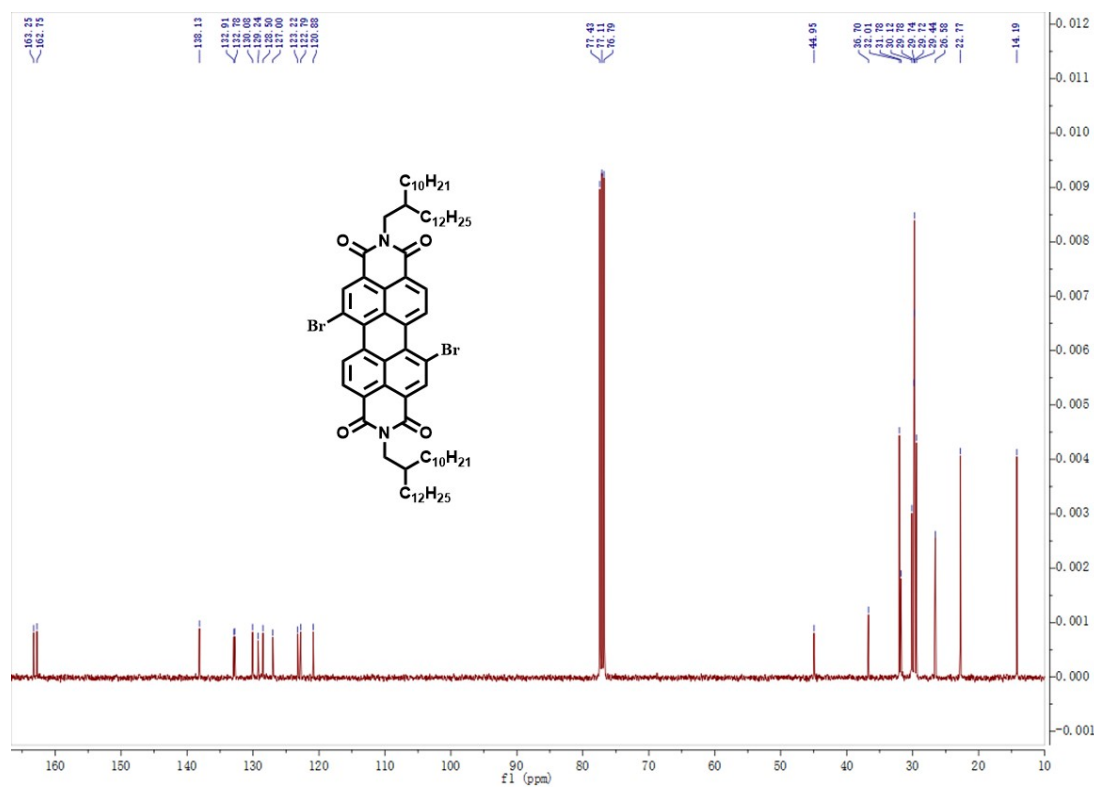


Figure S19: ^{13}C NMR spectrum of 1,7-diBr-PDI in CDCl_3 at 298 K.

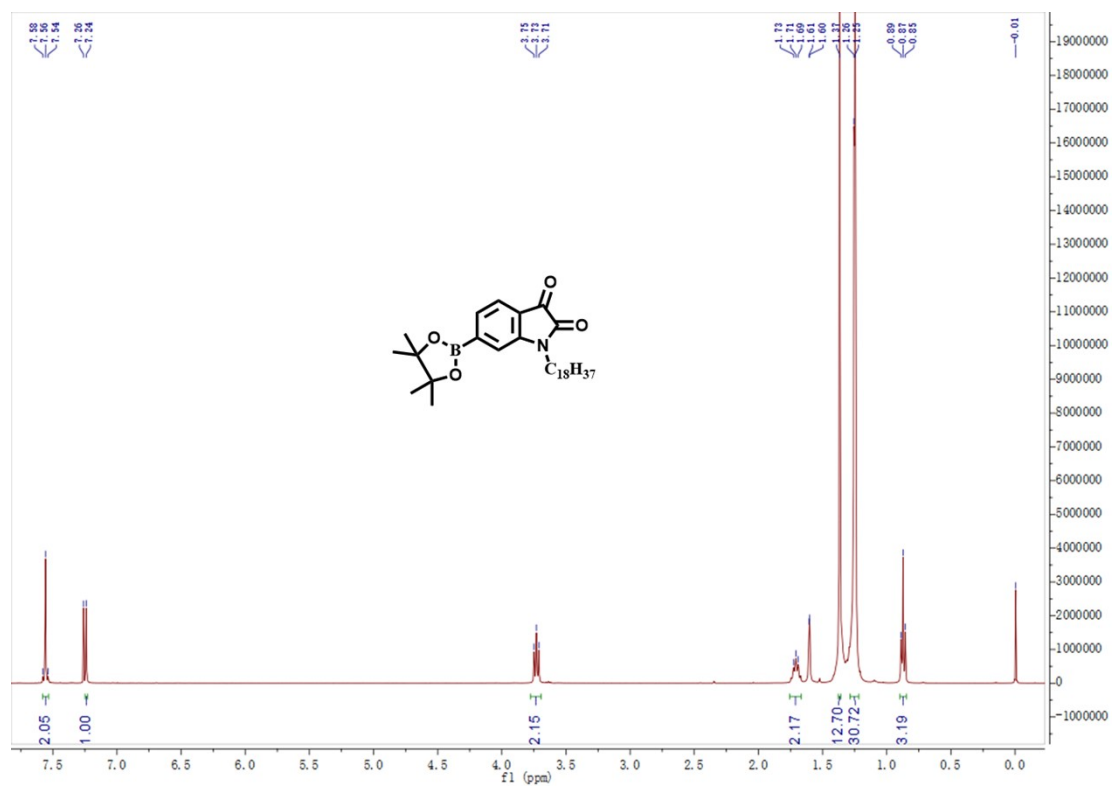


Figure S20: ^1H NMR spectrum of IS-B in CDCl_3 at 298 K.

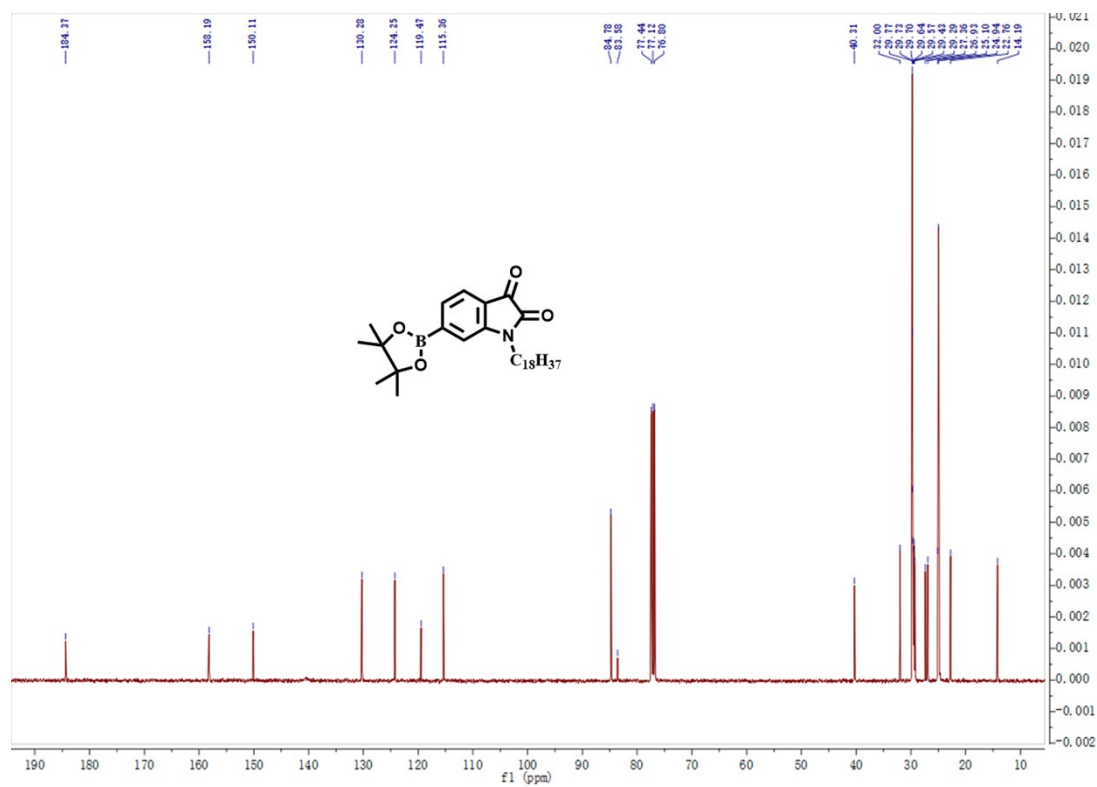


Figure S21: ^{13}C NMR spectrum of IS-B in CDCl_3 at 298 K.

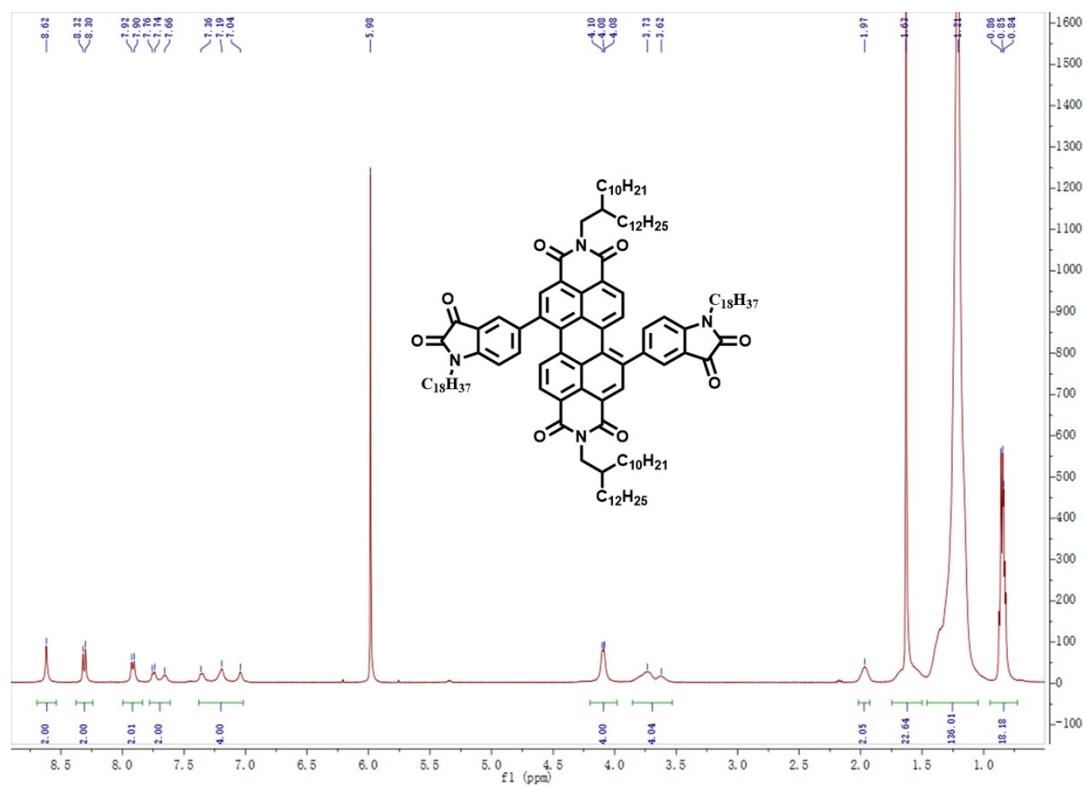


Figure S22: ^1H NMR spectrum of PDI-DIIS in $\text{CDCl}_2\text{CDCl}_2$ at 298 K.

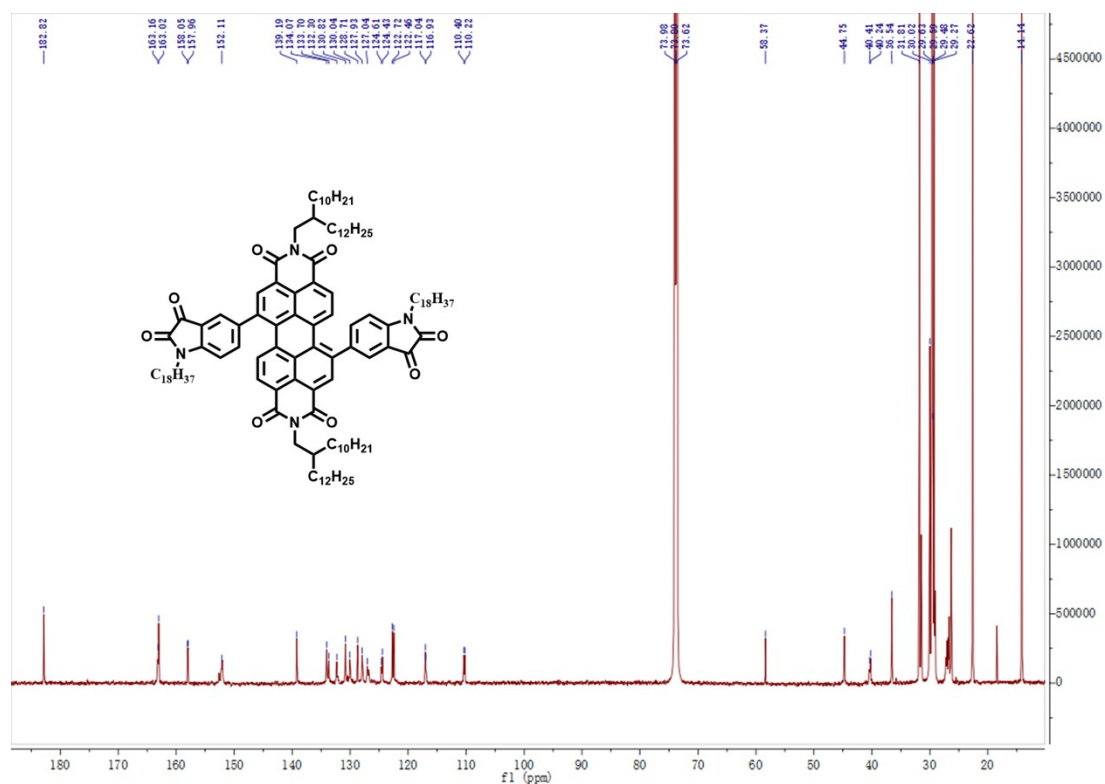


Figure S23: ^{13}C NMR spectrum of PDI-DIIS in $\text{CDCl}_2/\text{CDCl}_2$ at 298 K.

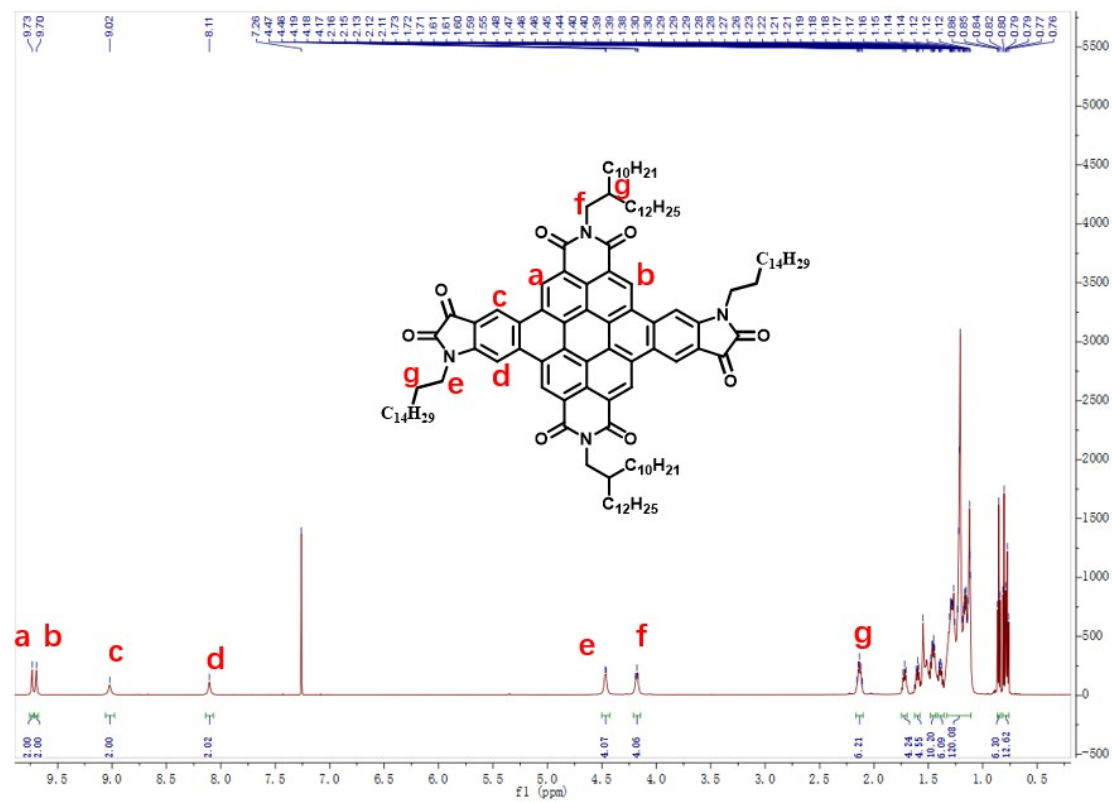


Figure S24: ^1H NMR spectrum of FPDI-DIIS in CDCl_3 at 323 K.

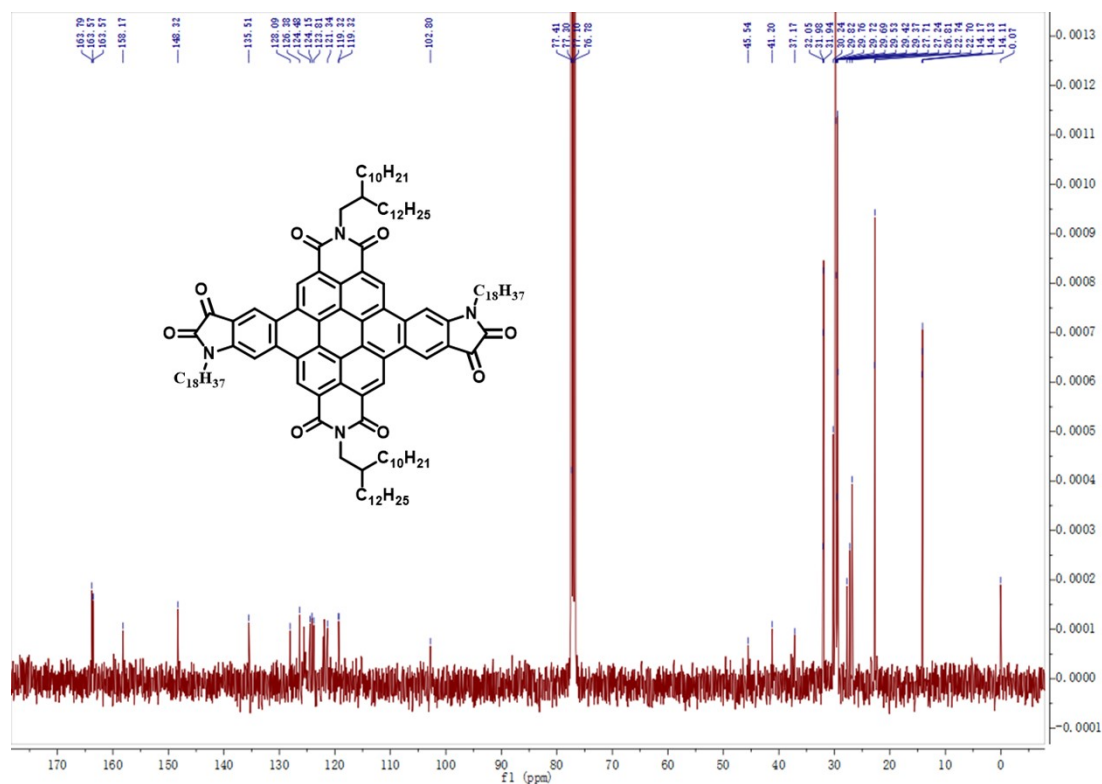


Figure S25: ¹³C NMR spectrum of FPDI-DIIS in CDCl₃ at 298 K.

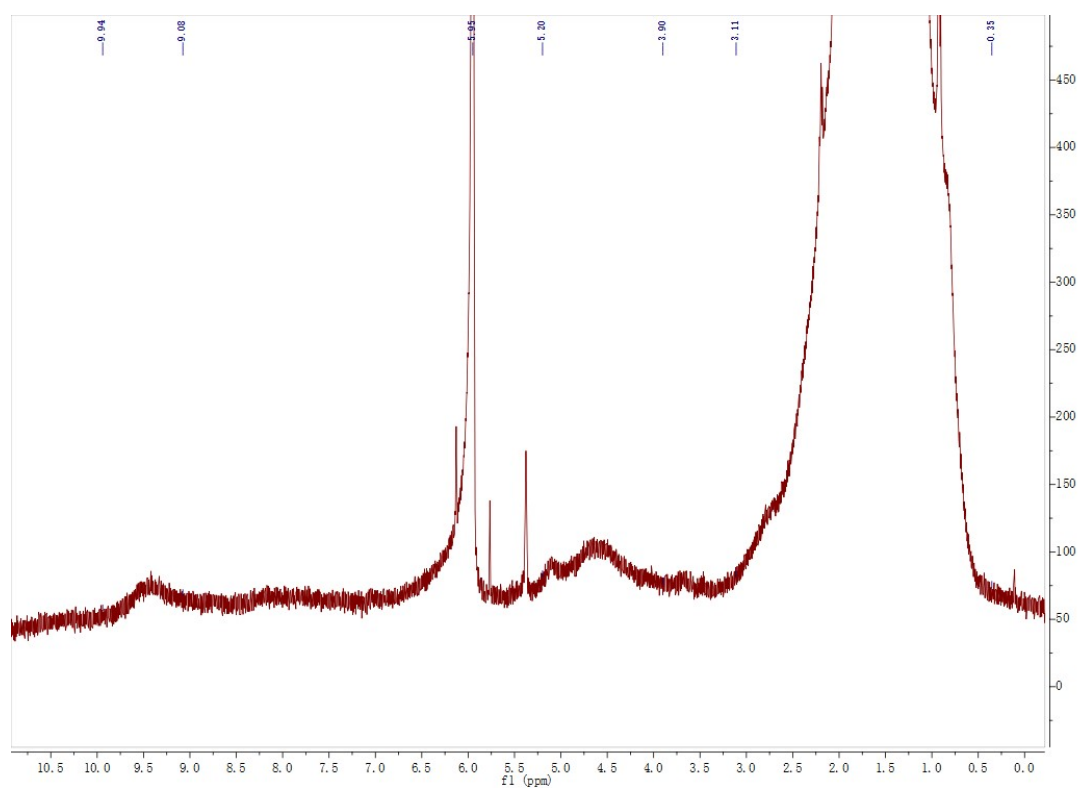


Figure S26: ¹H NMR spectrum of PB in CDCl₂CDCl₂ at 403 K.

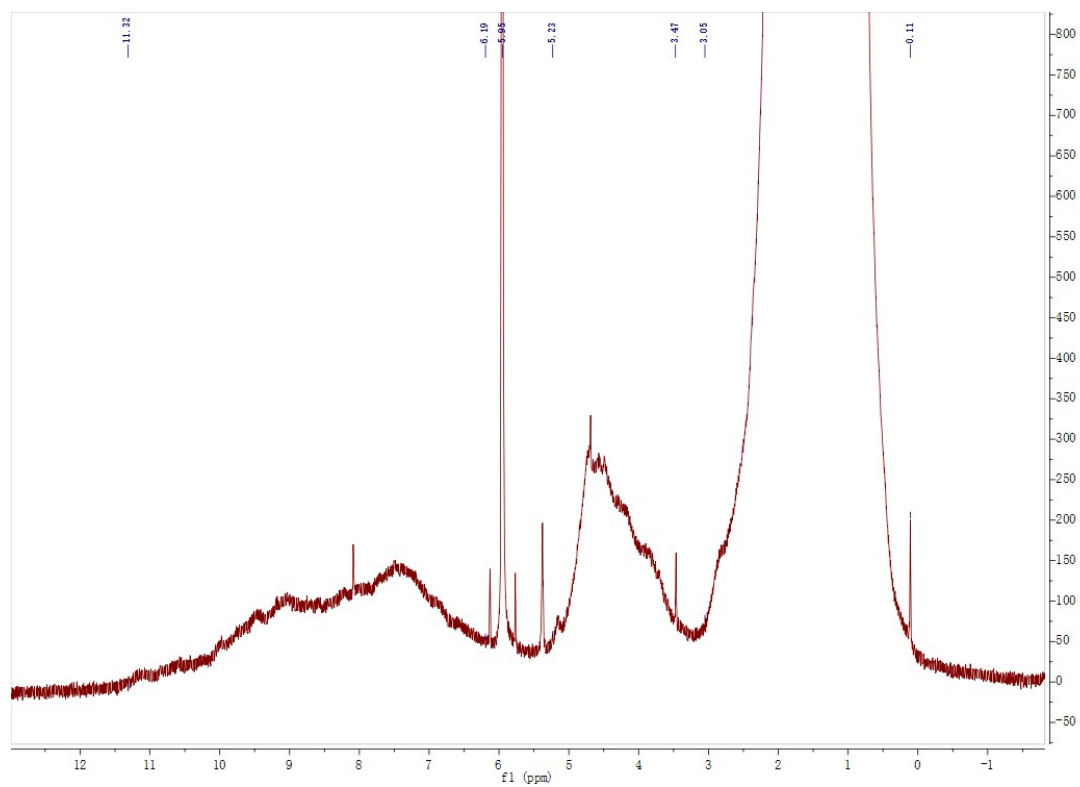


Figure S27: ^1H NMR spectrum of PN in $\text{CDCl}_2/\text{CDCl}_2$ at 403 K.

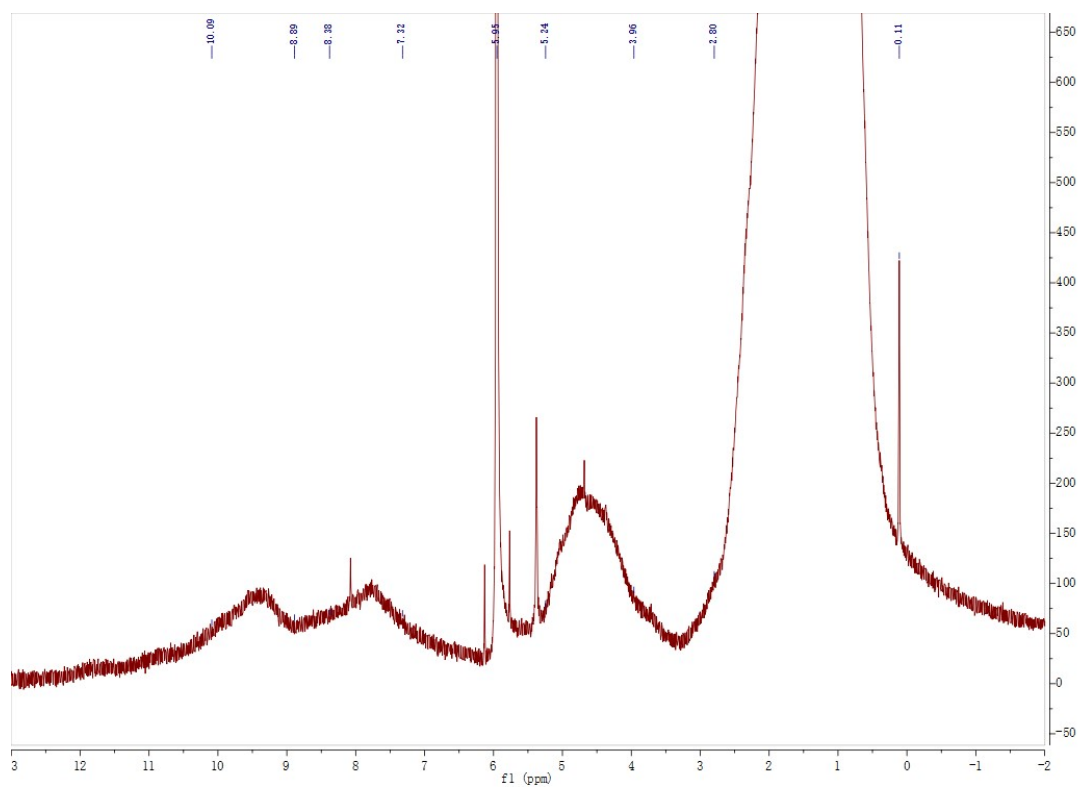


Figure S28: ^1H NMR spectrum of PD in $\text{CDCl}_2/\text{CDCl}_2$ at 403 K.

10. MS spectra

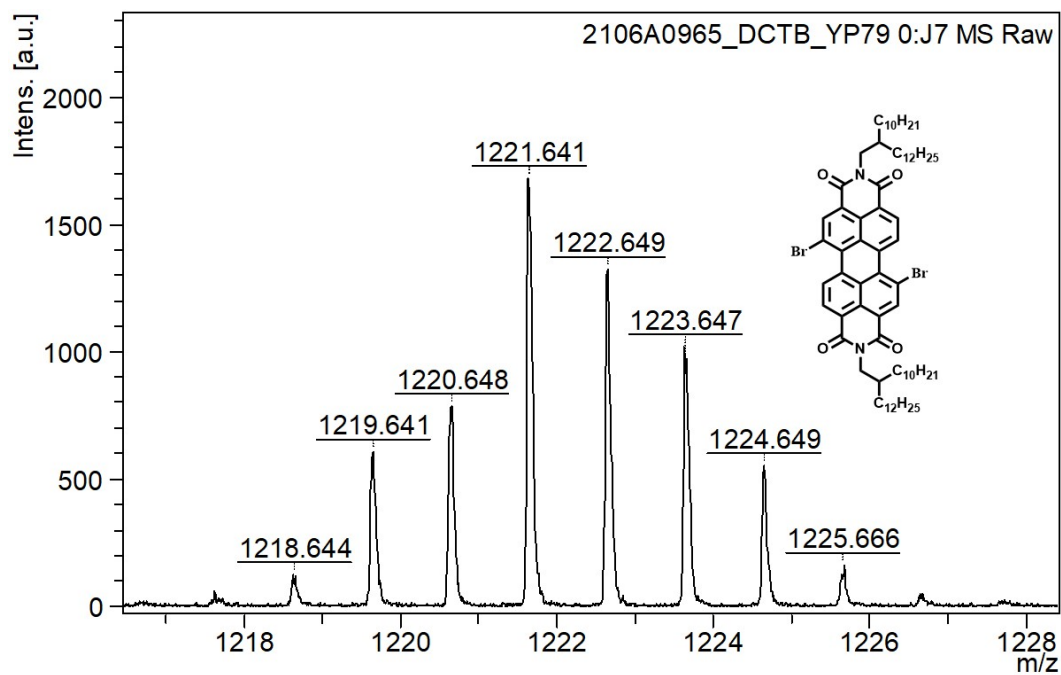


Figure S29: MS spectra of 1,7-diBr-PDI.

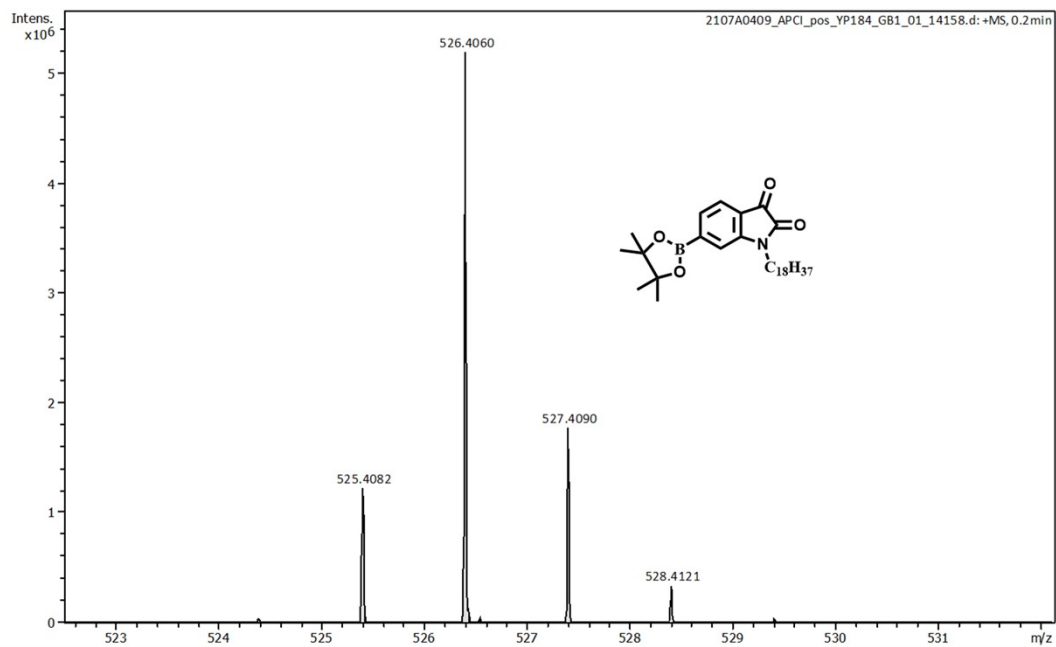


Figure S30: MS spectra of IS-B.

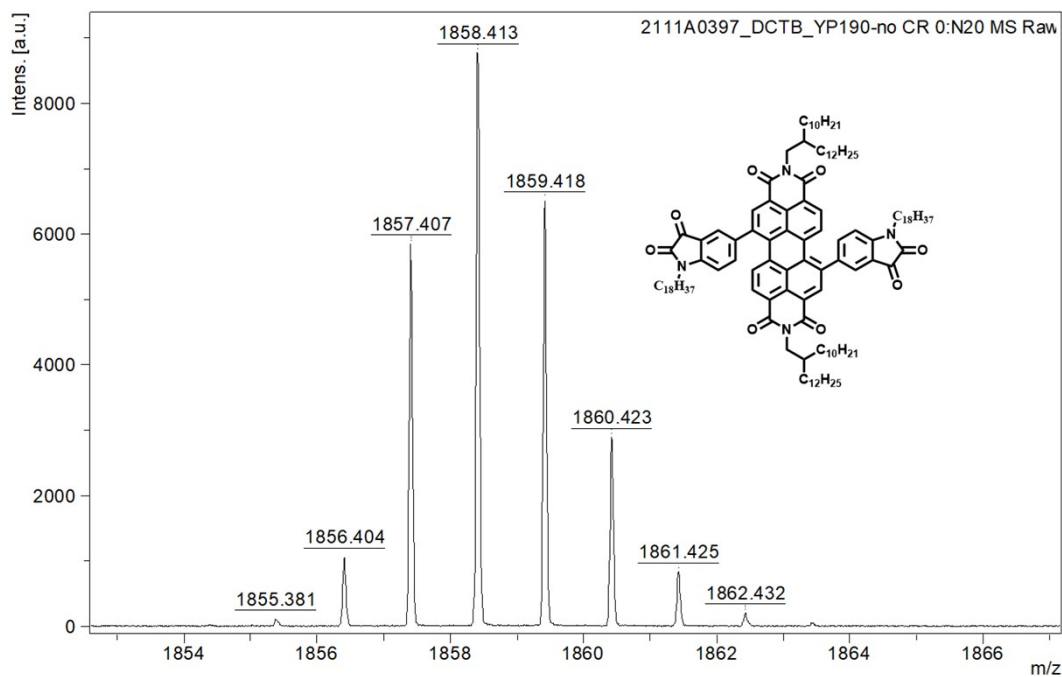


Figure S31: MS spectra of PDI-DIIS.

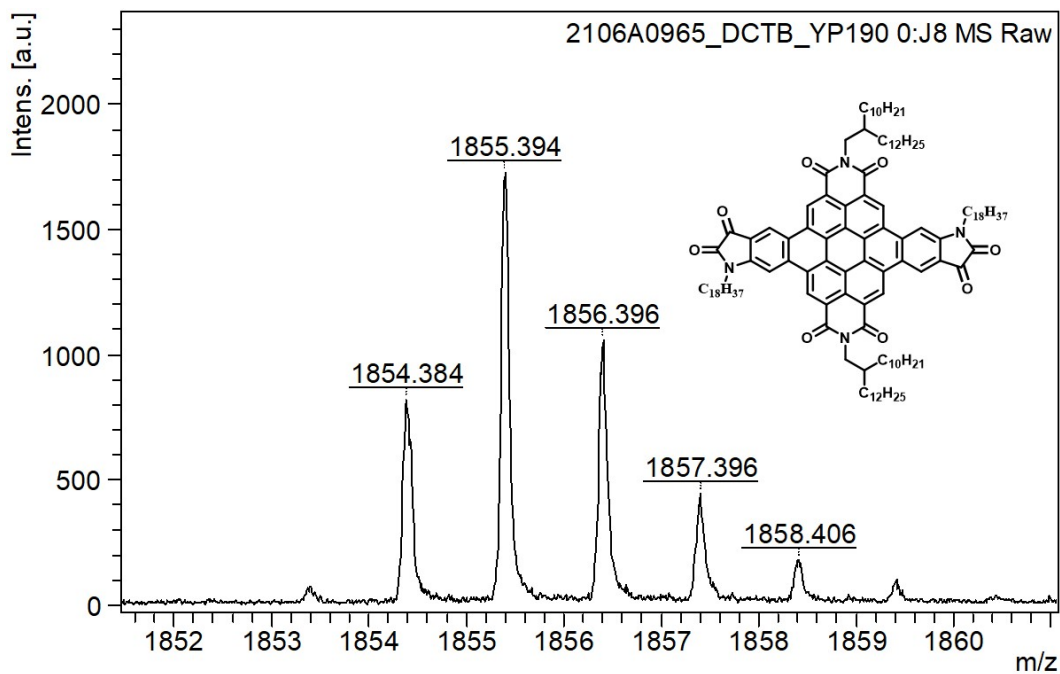


Figure S32: MS spectra of FPDI-DIIS.

11. References

- 1 S. Sengupta, R. K. Dubey, R. W. M. Hoek, S. P. P. van Eeden, D. D. Gunbas, F. C. Grozema, E. J. R. Sudholter, and W. F. Jager, *J. Org. Chem.*, 2014, **79**, 6655.
- 2 N. M. Randell, C. L. Radford, J. Yang, J. Quinn, D. Hou, Y. Li, and T. L. Kelly, *Chem. Mater.*, 2018, **30**, 4864.
- 3 Y. He, H. Liao, S. Lyu, X. Xu, Z. Li, I. McCulloch, W. Yue and Y. Wang, *Chem. Sci.*, 2021, **12**, 5177.
- 4 A. Faurie, F. Gohier and P. Frère, *Dyes and Pigments*, 2018, **154**, 38.
- 5 Y. Deng, B. Sun, Y. He, J. Quinn, C. Guo and Y. Li, *Chem. Commun.*, 2015, **51**, 13515.